Monthly Notices
of the
ROYAL ASTRONOMICAL SOCIETY

MNRAS **490,** 1479–1487 (2019)
Advance Access publication 2019 September 30

doi:10.1093/mnras/stz2713

WASP-South hot Jupiters: WASP-178b, WASP-184b, WASP-185b, and WASP-192b

Coel Hellier,[1]★ D. R. Anderson,[1,2] K. Barkaoui,[3,4] Z. Benkhaldoun,[3] F. Bouchy,[5] A. Burdanov,[6] A. Collier Cameron,[7] L. Delrez,[6,8] M. Gillon,[6] E. Jehin,[6] L. D. Nielsen,[5] P. F. L. Maxted,[1] F. Pepe,[5] D. Pollacco,[2] F. J. Pozuelos,[4,6] D. Queloz,[8] D. Ségransan,[5] B. Smalley,[1] A. H. M. J. Triaud,[9] O. D. Turner,[1,5] S. Udry[5] and R. G. West[2]

[1]*Astrophysics Group, Keele University, Staffordshire ST5 5BG, UK*
[2]*Department of Physics, University of Warwick, Gibbet Hill Road, Coventry CV4 7AL, UK*
[3]*Oukaimeden Observatory, High Energy Physics and Astrophysics Laboratory, Cadi Ayyad University, Marrakech, Morocco*
[4]*Astrobiology Research Unit, Université de Liège, Liège 1, Belgium*
[5]*Observatoire astronomique de l'Université de Genève, 51 Chemin des Maillettes, CH-1290 Sauverny, Switzerland*
[6]*Space sciences, Technologies and Astrophysics Research (STAR) Institute, Université de Liège, Liège 1, Belgium*
[7]*SUPA, School of Physics and Astronomy, University of St. Andrews, North Haugh, Fife KY16 9SS, UK*
[8]*Cavendish Laboratory, J J Thomson Avenue, Cambridge CB3 0HE, UK*
[9]*School of Physics and Astronomy, University of Birmingham, Edgbaston, Birmingham B15 2TT, UK*

Accepted 2019 September 23. Received 2019 September 11; in original form 2019 July 29

ABSTRACT

We report on four new transiting hot Jupiters discovered by the WASP-South survey. WASP-178b transits a $V = 9.9$, A1V star with $T_{\rm eff} = 9350 \pm 150$ K, the second-hottest transit host known. It has a highly bloated radius of $1.81 \pm 0.09\ R_{\rm Jup}$, in line with the known correlation between high irradiation and large size. With an estimated temperature of 2470 ± 60 K, the planet is one of the best targets for studying ultrahot Jupiters that is visible from the Southern hemisphere. The three host stars WASP-184, WASP-185, and WASP-192 are all post-main-sequence G0 stars of ages 4–8 Gyr. The larger stellar radii (1.3–1.7 $M_\odot$) mean that the transits are relatively shallow (0.7–0.9 per cent) even though the planets have moderately inflated radii of 1.2–1.3 $R_{\rm Jup}$. WASP-185b has an eccentric orbit ($e = 0.24$) and a relatively long orbital period of 9.4 d. A star that is 4.6 arcsec from WASP-185 and 4.4 mag fainter might be physically associated.

Key words: stars: individual: WASP-178 – stars: individual: WASP-184 – stars: individual: WASP-185 – stars: individual: WASP-192 – planetary systems.

1 INTRODUCTION

Since its start in 2006 May the WASP-South survey for transiting exoplanets operated until mid-2016, obtaining data on over 2500 nights and recording 400 billion photometric data points on 10 million stars. From 2006 to mid-2012 WASP-South used 200-mm, f/1.8 lenses, searching for transits of stars of $V = 9$–13, and obtaining typically 20 000 data points on each star. Coverage adds up to the whole sky between declination +8° and –70°, other than the crowded galactic plane, with each field being observed in typically three or four different years. In mid-2012 WASP-South switched to 85-mm, f/1.2 lenses, changing the useful magnitude range to $V = 6.5$–11.5, with the aim of finding the very brightest hot-Jupiter hosts such as WASP-189 (Anderson et al. 2018).

WASP-South transit candidates proved well matched to follow-up with the 1.2-m Euler Telescope and CORALIE spectrograph, teamed with the TRAPPIST-South photometric telescope and (more recently) TRAPPIST-North, which together observed 1600 planet candidates. So far WASP-South has led to the announcement of 154 transiting exoplanets (34 of them jointly with data from WASP-South's northern counterpart, SuperWASP).[1]

Follow-up of WASP-South candidates is now nearing completion, and in any case such surveys are rapidly being superseded by the space-based *Transiting Exoplanet Survey Satellite* (*TESS*)

★ E-mail: c.hellier@keele.ac.uk

[1] See https://wasp-planets.net

Table 1. Observations.

Facility	Date	Notes
WASP-178		
WASP-South	2006 May–2014 Aug	101 600 points
CORALIE	2017 Apr–2018 July	23 RVs
EulerCAM	2018 Mar 26	*I* filter
WASP-184		
WASP-South	2007 Feb–2012 July	24 300 points
CORALIE	2015 June–2018 July	19 RVs
TRAPPIST-South	2016 Mar 5	Blue-block
EulerCAM	2018 Apr 2, 11	*R* filter
WASP-185		
WASP-South	2006 May–2012 June	34 000 points
CORALIE	2015 June–2018 Aug	24 RVs
TRAPPIST-South	2014 Apr 9	*z* band
TRAPPIST-North	2019 June 9	*z* band
WASP-192		
WASP-South	2006 May–2012 July	42 200 points
CORALIE	2016 June–2019 Apr	12 RVs
TRAPPIST-South	2016 Apr 17	Blue-block
TRAPPIST-South	2019 June 6	$I + z$ band

survey (Ricker et al. 2016). We report here four new transiting hot Jupiters. While WASP-184b and WASP-192b are routine hot Jupiters transiting fainter, $V = 12$, stars, WASP-178b transits a bright A1V star that is the hottest of the WASP planet hosts, while WASP-185b has an eccentric, 9.4-d orbit.

2 OBSERVATIONS

The WASP-South photometry was accumulated into multiyear light curves for every catalogued star, which were then searched for transits using automated routines (Pollacco et al. 2006; Collier Cameron et al. 2007b), followed by human vetting of the search outputs. Planet candidates were then listed for follow-up observations by the TRAPPIST-South 0.6-m robotic photometer (e.g. Gillon et al. 2013) and the Euler/CORALIE spectrograph (e.g. Triaud et al. 2013). Transit photometry for the stars reported here was also obtained with the EulerCAM photometer (e.g. Lendl et al. 2012) and with TRAPPIST-North (Barkaoui et al. 2019). Our observations are listed in Table 1.

For three of our stars (WASP-184, WASP-185, and WASP-192) the CORALIE spectra were reduced to radial velocity (RV) measurements using a standard G2 mask (Pepe et al. 2002), while for the hotter star WASP-178 we used an A0 mask. The resulting values are listed in Table A1.

As we routinely do for WASP-South planet discoveries, we used the WASP photometry, typically spanning 6 months of observation in a year and several years of coverage, to look for rotational modulations of the planet-host stars. Our methods are detailed in Maxted et al. (2011). For the four stars reported here we found no significant modulations with upper limits of 1–2 mmag (as reported in the tables for each star).

3 SPECTRAL ANALYSES

We combined the CORALIE spectra for each object in order to make a spectral analysis. For three of the stars discussed here (WASP-184, WASP-185, and WASP-192) we adopt the same methods used in recent WASP-South papers (e.g. Hellier et al. 2019a), as described by Doyle et al. (2013). Thus we estimated the effective temperature, $T_{\rm eff}$, from the Hα line, and the surface gravity, $\log g$, from Na I D and Mg I b lines. We also translate the $T_{\rm eff}$ value to give an indicative spectral type. To estimate the metallicity, [Fe/H], we make equivalent width measurements of unblended Fe I lines, quoting errors that take account of the uncertainties in $T_{\rm eff}$ and $\log g$. We use the same Fe I lines to measure $v \sin i$ values, taking into account the CORALIE instrumental resolution ($R = 55\,000$) and adopting macroturbulence values from Doyle et al. (2014). The spectral analysis values are reported in the tables for each star.

WASP-178 is much hotter than the above stars, with $T_{\rm eff} = 9350 \pm 150$ K. For this star we measured over 100 clean, unblended, Fe I and Fe II lines in the spectral range 500–600 nm. The stellar parameters of $T_{\rm eff}$, $\log g$, and microturbulence were obtained by iteratively adjusting them, using non-linear least squares, in order to find the values that minimized the scatter in the abundance obtained from the Fe lines. This procedure simultaneously attempts to remove any trends in abundance with excitation potential (temperature diagnostic) and equivalent width (microturbulence diagnostic), as well as any differences between the Fe I and Fe II lines (surface gravity diagnostic). The parameter uncertainties were obtained from the residual scatter in the optimal solution (see Niemczura, Smalley & Pych 2014 for further discussion on stellar parameter determination).

4 SYSTEM PARAMETERS

Our process for parametrizing the systems combines all our data, photometry and RV measurements, in one Markov chain Monte Carlo (MCMC) analysis, using a code developed in several iterations from that originally described by Collier Cameron et al. (2007a).

Our standard procedure (see e.g. Hellier et al. 2019a) places a Gaussian 'prior' on the stellar mass. We derive this using the stellar effective temperature and metallicity, from the spectral analysis, and an estimate of the stellar density, from initial analysis of the transit. These are used as inputs to the BAGEMASS code (Maxted, Serenelli & Southworth 2015), based on the GARSTEC stellar evolution code (Weiss & Schlattl 2008), which then outputs estimates for the stellar mass and age. WASP-178 is too hot for the BAGEMASS code to be reliable, so we instead adopted a mass prior of 2.04 ± 0.12 M$_\odot$, from expectations of a main-sequence star of its temperature (e.g. Boyajian et al. 2013), followed by checking that this models the transit to give a self-consistent set of parameters.

In more recent WASP-South papers, following the availability of *Gaia* Data Release 2 (DR2) parallaxes (Gaia Collaboration et al. 2016, 2018), we also place a prior on the stellar radius. We apply the Stassun & Torres (2018) correction to the parallax to produce a distance estimate, and then use the infrared flux method (Blackwell & Shallis 1977) to arrive at the stellar radius. Before the *Gaia* DR2, getting the stellar radius wrong was one of the commonest sources of systematic error in transit analyses, and thus a prior on the radius improves the reliability of the solution and can make up for limitations in the transit photometry (see e.g. Hellier et al. 2019b).

In modelling the RVs we first allowed an eccentric orbit (which is required for WASP-185), but where it was not required (the other three systems) we enforced a circular orbit (as discussed in Anderson et al. 2012, this makes use of the expectation that the time for tidal circularization of a hot-Jupiter orbit is often shorter than the time in its current orbit). To fit the transit photometry we adopted limb-darkening coefficients by interpolating from the four-parameter, non-linear law of Claret (2000), as appropriate for the star's temperature and metallicity. The WASP passband and the

Table 2. Bayesian mass and age estimates for the host stars using GARSTEC stellar models assuming $\alpha_{\rm MLT} = 1.78$. Columns 2, 3, and 4 give the maximum likelihood estimates of the age, mass, and initial metallicity, respectively. Columns 5 and 6 give the mean and standard deviation of their posterior distributions. The systematic errors on the mass and age due to uncertainties in the mixing length and helium abundance are given in columns 7–10.

Star	$\tau_{\rm iso,\,b}$ (Gyr)	$M_{\rm b}$ ($M_\odot$)	[Fe/H]$_{\rm i,\,b}$	$\langle\tau_{\rm iso}\rangle$ (Gyr)	$\langle M_\star\rangle$ ($M_\odot$)	$\sigma_{\tau,\,Y}$	$\sigma_{\tau,\,\alpha}$	$\sigma_{M,\,Y}$	$\sigma_{M,\,\alpha}$
WASP-184	4.0	1.29	+0.168	4.66 ± 1.15	1.245 ± 0.072	−0.13	0.40	−0.036	−0.005
WASP-185	7.2	1.09	+0.066	6.63 ± 1.58	1.116 ± 0.068	0.23	1.87	−0.048	−0.069
WASP-192	5.1	1.16	+0.215	5.70 ± 1.92	1.137 ± 0.069	0.21	0.98	−0.043	−0.016

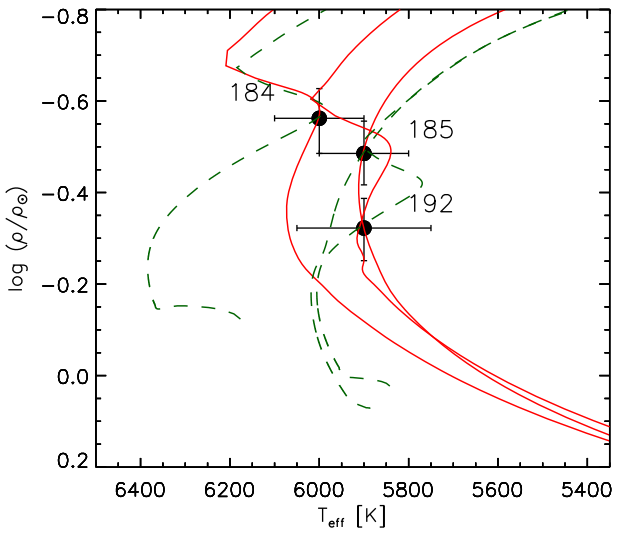

Figure 1. The host star's effective temperature ($T_{\rm eff}$) versus density, each symbol being labelled by the WASP planet number). We show best-fitting evolution tracks (green dashed lines) and isochrones (red solid lines) for the masses, ages, and [Fe/H] values listed in Table 2.

TRAPPIST 'blue-block' filter are wide, non-standard passbands, for which we approximate by using *R*-band coefficients, which is sufficient for the quality of our photometry. The MCMC code includes a step where the error bars are inflated such that the fit to each data set has a χ^2_ν of 1. This allows for red noise not accounted for in the input errors, thus balancing the different data sets and increasing the output error ranges. An account of the effects of red noise in typical WASP-planet discovery data sets is given in Smith et al. (2012).

The parameters resulting from the MCMC analysis are listed in the tables for each system. $T_{\rm c}$ is the mid-transit epoch, P is the orbital period, ΔF is the transit depth that would be observed in the absence of limb darkening, T_{14} is the duration from first to fourth contact, b the impact parameter, and K_1 the stellar reflex velocity. For WASP-184, WASP-185, and WASP-192 the BAGEMASS outputs are tabulated in Table 2, while the best-fitting stellar evolution tracks and isochrones are shown in Fig. 1 (WASP-178 is too hot for the BAGEMASS code to be reliable).

5 WASP-178

WASP-178 (=HD 134004) is a bright, $V = 9.95$, star for which the spectral analysis suggests $T_{\rm eff} = 9350 \pm 150$ K and an A1 IV–V classification (Table 3; Fig. 2). It appears to be a mild hot Am star, slightly enhanced in Fe ([Fe/H] = +0.21 ± 0.16) and slightly depleted in Ca and Sc ([Ca/H] = –0.06 ± 0.14, [Sc/H] = –0.35 ± 0.08). Y and Ba are also enhanced by +0.35 ± 0.10 and +0.96 ± 0.15, respectively. Interstellar Na D lines lead to an

Table 3. System parameters for WASP-178.

1SWASP J150904.89−424217.7
HD 134004; 2MASS 15090488–4242178
Gaia RA = $15^{\rm h}09^{\rm m}04^{\rm s}.89$, Dec. = –42°42′17″.8 (J2000)
V mag = 9.95; *Gaia* G = 9.91; J = 9.77
Rotational modulation: <1.5 mmag
Gaia DR2 pm (RA) –10.01 ± 0.12, (Dec.) –5.65 ± 0.10 mas yr^{-1}
Gaia DR2 parallax: 2.3119 ± 0.0600 mas
Distance = 418 ± 16 pc

Stellar parameters from spectroscopic analysis

Spectral type	A1 IV–V
$T_{\rm eff}$ (K)	9350 ± 150
log g	4.35 ± 0.15
v sin i (km s^{-1})	8.2 ± 0.6
Microturbulence (km s^{-1})	2.9 ± 0.2
[Fe/H]	+0.21 ± 0.16
[Ca/H]	–0.06 ± 0.14
[Sc/H]	–0.35 ± 0.08
[Cr/H]	+0.43 ± 0.10
[Y/H]	+0.35 ± 0.10
[Ba/H]	+0.96 ± 0.15
[Ni/H]	+0.32 ± 0.12

Parameters from MCMC analysis

P (d)	3.3448285 ± 0.0000012
$T_{\rm c}$ (HJD) (UTC)	245 6927.06839 ± 0.00047
T_{14} (d)	0.1446 ± 0.0016
$T_{12} = T_{34}$ (d)	0.0197 ± 0.0016
$\Delta F = R_{\rm P}^2/R_*^2$	0.01243 ± 0.00028
b	0.54 ± 0.05
i (°)	85.7 ± 0.6
K_1 (km s^{-1})	0.139 ± 0.009
γ (km s^{-1})	− 23.908 ± 0.007
e	0 (adopted) (< 0.08 at 2σ)
a/R_*	7.17 ± 0.21
M_* ($M_\odot$)	2.07 ± 0.11
R_* ($R_\odot$)	1.67 ± 0.07
log g_* (cgs)	4.31 ± 0.04
ρ_* ($\rho_\odot$)	0.44 ± 0.05
$T_{\rm eff}$ (K)	9360 ± 150
$M_{\rm P}$ ($M_{\rm Jup}$)	1.66 ± 0.12
$R_{\rm P}$ ($R_{\rm Jup}$)	1.81 ± 0.09
log $g_{\rm P}$ (cgs)	3.07 ± 0.05
$\rho_{\rm P}$ ($\rho_{\rm J}$)	0.28 ± 0.05
a (au)	0.0558 ± 0.0010
$T_{\rm P,\,A\,=\,0}$ (K)	2470 ± 60

Priors were $M_* = 2.04 \pm 0.12$ $M_\odot$ and $R_* = 1.81 \pm 0.12$ $R_\odot$
Errors are 1σ; Limb-darkening coefficients were
*R*band: $a_1 = 0.669$, $a_2 = -0.223$, $a_3 = 0.280$, $a_4 = -0.125$
*I*band: $a_1 = 0.724$, $a_2 = -0.616$, $a_3 = 0.644$, $a_4 = -0.245$

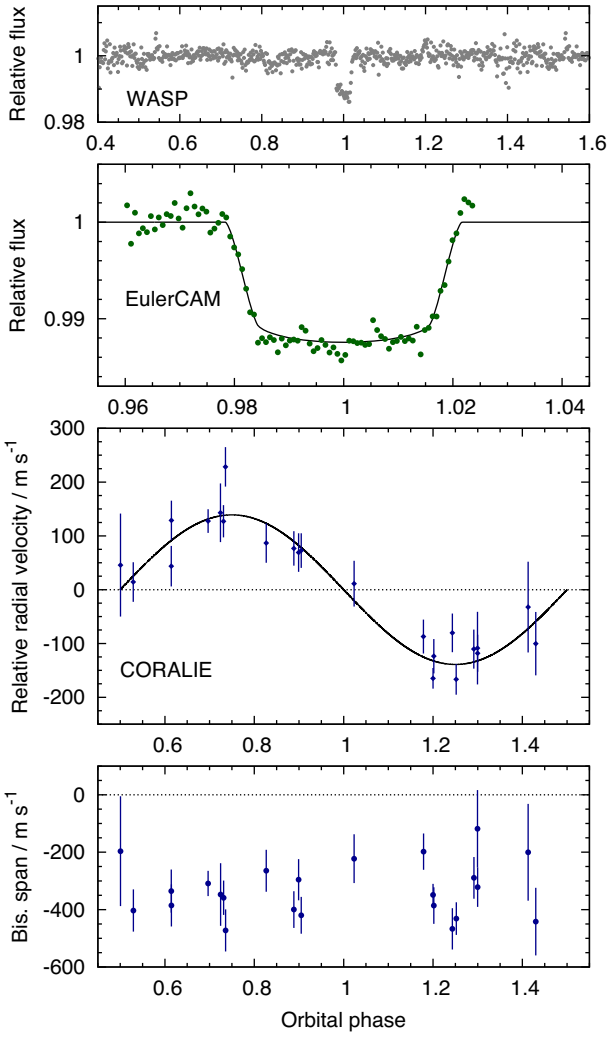

Figure 2. WASP-178b discovery data. Top: the WASP data folded on the transit period. Second panel: the EulerCAM transit light curve together with the fitted MCMC model. Third panel: the CORALIE RV data and fitted model. Bottom: the bisector spans of the CORALIE data.

estimate of $E(B-V) = 0.06 \pm 0.01$, which then implies (through the infrared flux method) a $T_{\rm eff}$ of 9390 ± 190 K, consistent with that from the spectral analysis. The projected rotation speed is relatively low at $v \sin i = 8.2 \pm 0.6$ km s^{-1} (measured assuming zero macroturbulence). We report (Table 3) a stellar mass of 2.07 ± 0.11 $M_\odot$ and a stellar radius of 1.67 ± 0.07 $R_\odot$, which are compatible with a main-sequence, non-evolved status.

WASP-178 appears to be relatively isolated on the sky, with no nearby stars within 17 arcsec listed in *Gaia* DR2, and all stars within 30 arcsec being >7 mag fainter. However, WASP-178 is noted in *Gaia* DR2 as having significant excess noise in the astrometry, amounting to 0.18 mas in 254 astrometric observations. This could indicate an unresolved and unseen binary companion.

With a temperature of 9350 ± 150 K, WASP-178 is the second hottest known host of a hot Jupiter, behind the A0 star KELT-9 (Gaudi et al. 2017) at 10 170 K and ahead of the A2 star MASCARA-2/KELT-20 (Lund et al. 2017; Talens et al. 2018) at 8980 K.

Despite the high stellar temperature, CORALIE RVs are able to detect the orbital motion. The planet is in a 3.3-d orbit with a mass of 1.66 ± 0.12 $M_{\rm Jup}$ and a bloated radius of 1.81 ± 0.09 $R_{\rm Jup}$. The

Table 4. System parameters for WASP-184.

1SWASP J135804.10–302053.0	
2MASS 13580408–3020532	
Gaia RA = 13$^{\rm h}$58$^{\rm m}$04$^{\rm s}$.09, Dec. = –30°20′53″.3 (J2000)	
V mag = 12.9; *Gaia* G = 12.57; J = 11.6	
Rotational modulation: <2 mmag	
Gaia DR2 pm (RA) –4.36 ± 0.06, (Dec.) –5.09 ± 0.06 mas yr^{-1}	
Gaia DR2 parallax: 1.480 ± 0.037 mas	
Distance = 640 ± 28 pc	
Stellar parameters from spectroscopic analysis	
Spectral type	G0
$T_{\rm eff}$ (K)	6000 ± 100
log g	4.0 ± 0.2
$v \sin i$ (km s^{-1})	4.5 ± 1.1
[Fe/H]	+0.12 ± 0.08
log A(Li)	2.04 ± 0.08
Parameters from MCMC analysis	
P (d)	5.18170 ± 0.00001
$T_{\rm c}$ (HJD) (UTC)	245 7630.008 ± 0.001
T_{14} (d)	0.1990 ± 0.0027
$T_{12} = T_{34}$ (d)	0.0187 ± 0.0024
$\Delta F = R_{\rm P}^2/R_*^2$	0.0069 ± 0.0003
b	0.44 ± 0.14
i (°)	86.9 ± 1.1
K_1 (km s^{-1})	0.058 ± 0.010
γ (km s^{-1})	8.366 ± 0.008
e	0 (adopted) (< 0.25 at 2σ)
a/R_*	8.19 ± 0.42
M_* ($M_\odot$)	1.23 ± 0.07
R_* ($R_\odot$)	1.65 ± 0.09
log g_* (cgs)	4.09 ± 0.05
ρ_* ($\rho_\odot$)	0.27 ± 0.05
$T_{\rm eff}$ (K)	6000 ± 100
$M_{\rm P}$ ($M_{\rm Jup}$)	0.57 ± 0.10
$R_{\rm P}$ ($R_{\rm Jup}$)	1.33 ± 0.09
log $g_{\rm P}$ (cgs)	2.87 ± 0.10
$\rho_{\rm P}$ ($\rho_{\rm J}$)	0.24 ± 0.07
a (au)	0.0627 ± 0.0012
$T_{\rm P,\,A\,=\,0}$ (K)	1480 ± 50

Priors were $M_* = 1.25 \pm 0.07$ $M_\odot$ and $R_* = 1.59 \pm 0.10$ $R_\odot$
Errors are 1σ; Limb-darkening coefficients were
Rband: $a_1 = 0.578$, $a_2 = 0.022$, $a_3 = 0.359$, $a_4 = -0.230$

estimated equilibrium temperature is 2470 ± 60 K, the hottest of any planet with an orbital period of >3 d. Fig. 2 shows the transit photometry and RV orbit. We also plot the bisector spans against phase, where the absence of a correlation is a check against transit mimics (e.g. Queloz et al. 2001).

6 WASP-184

WASP-184 is a V = 12.9, G0 star with a metallicity of [Fe/H] = + 0.12 ± 0.08 and a distance of 640 ± 28 pc (Table 4; Fig. 3). WASP-184 is relatively isolated with no stars recorded in *Gaia* DR2 within 10 arcsec, and only two stars (>6 mag fainter) within 30 arcsec. There is no excess astrometric noise recorded in DR2. The mass and radius of WASP-184 (1.23 ± 0.07 $M_\odot$ and 1.65 ± 0.09 $R_\odot$) imply that it is evolving off the main sequence. Using the BAGEMASS code we compute an age of 4.7 ± 1.1 Gyr. Lithium depletion to the measured value of log A(Li) = 2.04 ± 0.08 could take ∼5 Gyr according to table 3 of Sestito & Randich (2005), which is consistent with the BAGEMASS age.

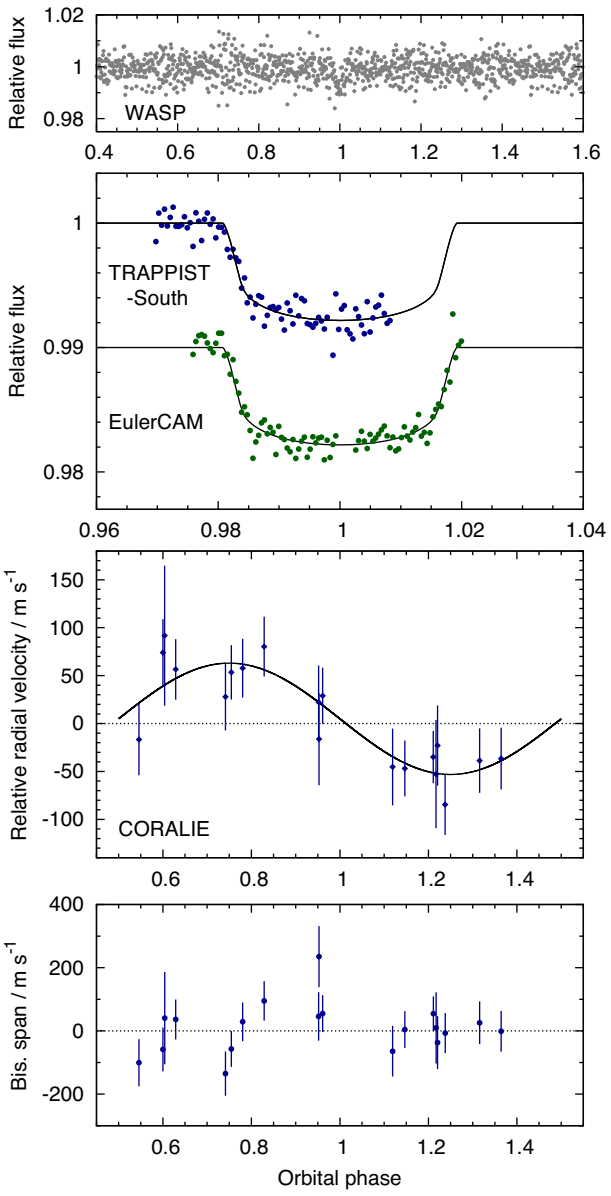

Figure 3. WASP-184b discovery data and fitted model, as for Fig. 2. The TRAPPIST, EulerCAM, and CORALIE observations are listed in Table 1.

The system is reasonably well parametrized by a partial transit from TRAPPIST-South, a nearly full transit from EulerCAM, and 19 RVs from CORALIE. The planet is in a 5.18-d orbit and is a moderately bloated, lower-mass hot Jupiter (0.57 ± 0.07 $M_{\rm Jup}$; 1.33 ± 0.09 $R_{\rm Jup}$).

7 WASP-185

WASP-185 is a $V = 11.1$, G0 star with a solar metallicity ([Fe/H] = –0.02 ± 0.06) at a distance of 275 ± 6 pc (Table 5; Fig. 4). It has an apparent companion star 4.6 arcsec away and 4.4 mag fainter in *Gaia G* (too faint for *Gaia* to report its proper motion, so we do not know whether the two are physically associated; at the distance of WASP-185 the separation would correspond to 1200 au). Otherwise WASP-185 is relatively isolated (with three other stars, >9 mag fainter, between 20 and 30 arcsec away). There is no DR2 excess astrometric noise reported for WASP-185. The companion star is sufficiently

Table 5. System parameters for WASP-185.

1SWASP J141614.30–193232.1	
2MASS 14161431–1932321	
Gaia RA = $14^{\rm h}16^{\rm m}14\overset{\rm s}{.}31$, Dec. = –19°32′32.″2 (J2000)	
V mag = 11.1; *Gaia* G = 10.89; J = 9.87	
Rotational modulation: <1 mmag	
Gaia DR2 pm (RA) –13.40 ± 0.08, (Dec) –6.06 ± 0.07 mas yr^{-1}	
Gaia DR2 parallax: 3.552 ± 0.043 mas	
Distance = 275 ± 6 pc	
Stellar parameters from spectroscopic analysis	
Spectral type	G0
$T_{\rm eff}$ (K)	5900 ± 100
log g	4.0 ± 0.2
$v \sin i$ (km s^{-1})	2.8 ± 0.9
[Fe/H]	–0.02 ± 0.06
log A(Li)	2.37 ± 0.09
Parameters from MCMC analysis	
P (d)	9.38755 ± 0.00002
$T_{\rm c}$ (HJD) (UTC)	245 6935.982 ± 0.002
T_{14} (d)	0.192 ± 0.006
$T_{12} = T_{34}$ (d)	0.040 ± 0.006
$\Delta F = R_{\rm P}^2/R_*^2$	0.0073 ± 0.0005
b	0.81 ± 0.03
i (°)	86.8 ± 0.3
K_1 (km s^{-1})	0.088 ± 0.004
γ (km s^{-1})	23.874 ± 0.003
e	0.24 ± 0.04
ω (°)	–42 ± 7
a/R_*	12.9 ± 0.7
M_* ($M_\odot$)	1.12 ± 0.06
R_* ($R_\odot$)	1.50 ± 0.08
log g_* (cgs)	4.13 ± 0.05
ρ_* ($\rho_\odot$)	0.33 ± 0.06
$T_{\rm eff}$ (K)	5900 ± 100
$M_{\rm P}$ ($M_{\rm Jup}$)	0.98 ± 0.06
$R_{\rm P}$ ($R_{\rm Jup}$)	1.25 ± 0.08
log $g_{\rm P}$ (cgs)	3.15 ± 0.07
$\rho_{\rm P}$ ($\rho_{\rm J}$)	0.50 ± 0.12
a (au)	0.0904 ± 0.0017
$T_{\rm P,\,A\,=\,0}$ (K)	1160 ± 35

Priors were $M_* = 1.11 \pm 0.06$ $M_\odot$ and $R_* = 1.58 \pm 0.09$ $R_\odot$
Errors are 1σ; Limb-darkening coefficients were
Rband: $a_1 = 0.568$, $a_2 = -0.009$, $a_3 = 0.443$, $a_4 = -0.271$
$z$band: $a_1 = 0.651$, $a_2 = -0.334$, $a_3 = 0.621$, $a_4 = -0.320$

distant that it will not affect the CORALIE RVs, however it is included in the extraction aperture for the TRAPPIST photometry. We therefore applied a correction of 1.8 per cent to the transit photometry, though in practice this amount is much less than the uncertainties.

The mass and radius of WASP-185 (1.12 ± 0.06 $M_\odot$ and 1.50 ± 0.08 $R_\odot$) indicate an evolved star, and the BAGEMASS code suggests an age of 6.6 ± 1.6 Gyr. Lithium depletion to the measured value of log A(Li) = 2.37 ± 0.09 could take ∼2 Gyr, but this abundance of lithium is found in NGC 188, which is ∼8 Gyr old according to table 3 of Sestito & Randich (2005). Thus the lithium is consistent with the BAGEMASS age.

We have only limited photometry of the transit, one ingress and one egress, both obtained in deteriorating observing conditions, and so the transit parametrization depends substantially on the stellar radius deduced from the *Gaia* DR2 distance. Our 24 CORALIE RVs trace out an eccentric orbit, though there is clearly additional

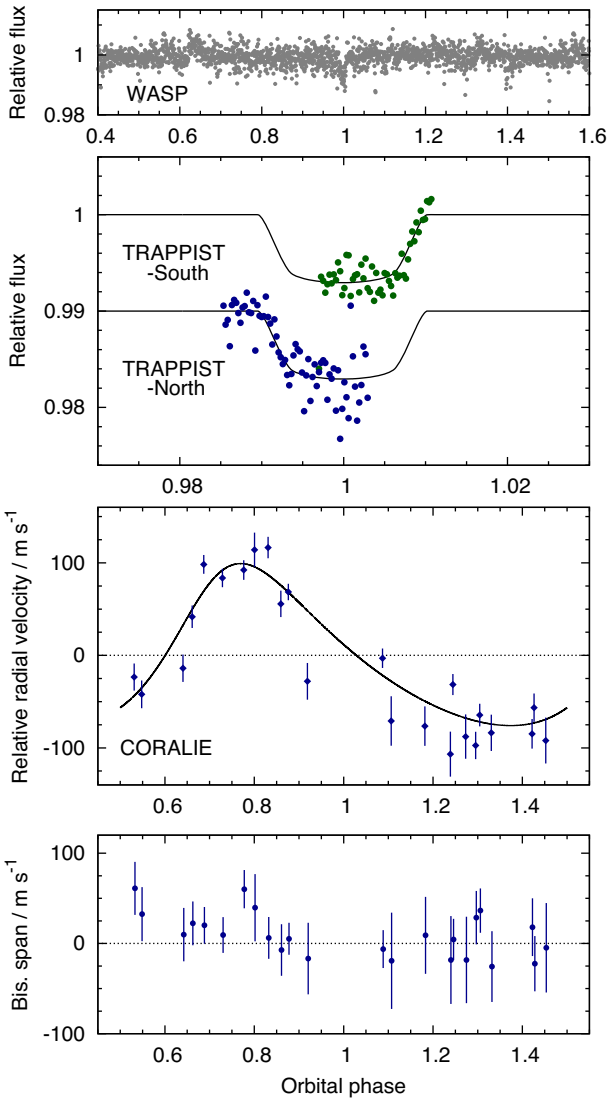

Figure 4. WASP-185b discovery data and fitted model, as for Figs 2 and 3.

scatter of unknown origin. This could be magnetic activity of the host star, though no rotational modulation is seen in the WASP data to a limit of 1 mmag (WASP-166 is an example of a system showing RV variation owing to magnetic activity, but no rotational modulation; Hellier et al. 2019b).

The planet's orbit has a relatively long period for a hot Jupiter, at 9.39 d, and has an eccentricity of $e = 0.24 \pm 0.04$. The impact factor is relatively high at $b = 0.81 \pm 0.03$. The planet's mass and radius ($0.98 \pm 0.06\ M_{\rm Jup}$ and $1.25 \pm 0.08\ R_{\rm Jup}$) are typical for hot Jupiters.

8 WASP-192

WASP-192 is a $V = 12.3$, G0 star with metallicity [Fe/H] $= +0.14 \pm 0.08$ at a distance of 495 ± 22 pc (Table 6; Fig. 5). It is isolated in the sky, with no stars, less than 6 mag fainter, within 30 arcsec according to *Gaia* DR2. There is no excess astrometric noise reported in DR2. The mass and radius ($1.09 \pm 0.06\ M_\odot$ and $1.32 \pm 0.07\ R_\odot$) indicate a moderately evolved star, and the BAGEMASS code produces an age of 5.7 ± 1.9 Gyr. Lithium depletion to the measured log A(Li) $= 2.11 \pm 0.13$ could take ~5 Gyr according to table 3 of Sestito & Randich (2005), which is consistent with the BAGEMASS age.

Table 6. System parameters for WASP-192.

1SWASP J145438.06–384439.6	
2MASS 14543809–3844403	
Gaia RA $= 14^{\rm h}54^{\rm m}38\overset{\rm s}{.}09$, Dec. $= -38^\circ44'40\overset{''}{.}3$ (J2000)	
V mag $= 12.3$; *Gaia* $G = 12.53$; $J = 11.5$	
Rotational modulation: <2 mmag	
Gaia DR2 pm (RA) 0.72 ± 0.07, (Dec.) -1.53 ± 0.06 mas yr^{-1}	
Gaia DR2 parallax: 1.939 ± 0.062 mas	
Distance $= 495 \pm 22$ pc	
Stellar parameters from spectroscopic analysis	
Spectral type	G0
$T_{\rm eff}$ (K)	5900 ± 150
log g	4.5 ± 0.2
$v \sin i$ (km s^{-1})	3.1 ± 1.1
[Fe/H]	$+0.14 \pm 0.08$
log A(Li)	2.11 ± 0.13
Parameters from MCMC analysis	
P (d)	2.8786765 ± 0.0000028
$T_{\rm c}$ (HJD) (UTC)	$245\,7271.3331 \pm 0.0017$
T_{14} (d)	0.0964 ± 0.0040
$T_{12} = T_{34}$ (d)	0.026 ± 0.004
$\Delta F = R_{\rm P}^2/R_*^2$	0.00926 ± 0.00061
b	0.84 ± 0.03
i ($^\circ$)	82.7 ± 0.6
K_1 (km s^{-1})	0.307 ± 0.017
γ (km s^{-1})	15.896 ± 0.013
e	0 (adopted) (< 0.25 at 2σ)
a/R_*	6.65 ± 0.34
M_* ($M_\odot$)	1.09 ± 0.06
R_* ($R_\odot$)	1.32 ± 0.07
log g_* (cgs)	4.236 ± 0.051
ρ_* ($\rho_\odot$)	0.476 ± 0.080
$T_{\rm eff}$ (K)	5910 ± 145
$M_{\rm P}$ ($M_{\rm Jup}$)	2.30 ± 0.16
$R_{\rm P}$ ($R_{\rm Jup}$)	1.23 ± 0.08
log $g_{\rm P}$ (cgs)	3.54 ± 0.07
$\rho_{\rm P}$ ($\rho_{\rm J}$)	1.22 ± 0.31
a (au)	0.0408 ± 0.0008
$T_{\rm P,\,A\,=\,0}$ (K)	1620 ± 60

Priors were $M_* = 1.09 \pm 0.06\ M_\odot$ and $R_* = 1.34 \pm 0.08\ R_\odot$
Errors are 1σ; Limb-darkening coefficients were
*R*band: $a_1 = 0.621$, $a_2 = -0.179$, $a_3 = 0.655$, $a_4 = -0.356$
*I*band: $a_1 = 0.697$, $a_2 = -0.435$, $a_3 = 0.801$, $a_4 = -0.394$

The planet WASP-192b has a typical hot-Jupiter orbit of $P = 2.88$ d with a relatively high impact parameter of $b = 0.84 \pm 0.03$. We have TRAPPIST photometry of one partial transit and one full transit, though that was in poorer observing conditions. The planet is more massive than average for a hot Jupiter at $2.30 \pm 0.16\ M_{\rm Jup}$, such that 12 CORALIE RVs show a well-defined orbital motion. The radius of $1.23 \pm 0.08\ R_{\rm Jup}$ is typical of hot Jupiters that have masses in the range 2–3 $M_{\rm Jup}$.

9 DISCUSSION

Recent papers have outlined a class of 'ultrahot Jupiters' (UHJs), defined by Parmentier et al. (2018) as Jupiters with day-side temperatures greater than 2200 K. Atmospheric characterization of UHJs such as WASP-18b, WASP-103b, and WASP-121b (e.g. Kreidberg et al. 2018a; Arcangeli et al. 2019) has revealed systematically

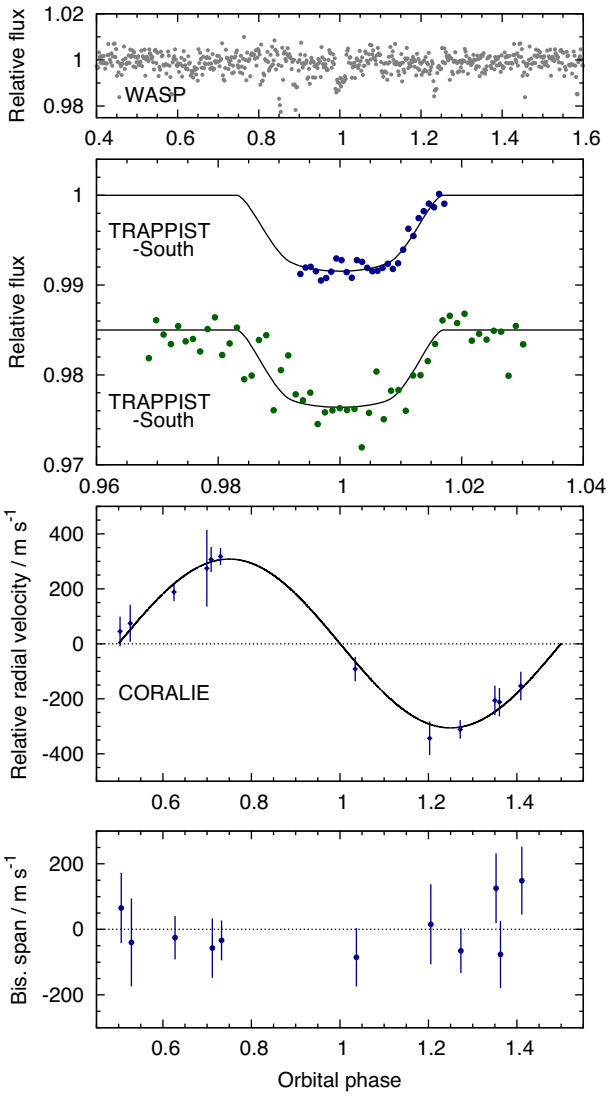

Figure 5. WASP-192b discovery data and fitted model, as for Figs 2 and 3.

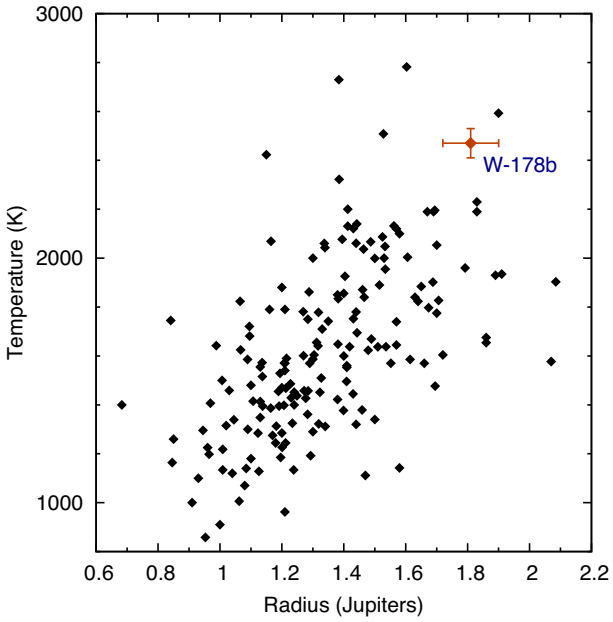

Figure 6. Radii and calculated temperatures of transiting hot Jupiters, showing the location of WASP-178b in red. KELT-9b is above the plot at 4600 K. The data are from http://exoplanet.eu. We caution about selection effects in such a plot since non-bloated planets would have shallower transits against larger, hotter stars, so would be harder to detect.

different behaviour from cooler planets. Whereas cooler planets can show strong water features (e.g. WASP-107b; Kreidberg et al. 2018b), water is thought to disassociate on the day-sides of UHJs, such that no water features are seen. The disassociated ions then drift to the night side, where they recombine. The molecule CO, however, has a stronger molecular bond, and is still present on the day sides of UHJs, where it can produce an emission feature (e.g. Parmentier et al. 2018).

In Table 7, we list the hottest of all the known UHJs, those with a calculated equilibrium temperature above 2300 K (the UHJ definition of *day-side* temperature > 2200 K includes many more objects than we list). We use equilibrium temperature, taking the

Table 7. The hottest of all known ultrahot Jupiters (UHJs).

Name	Eq. temp (K)	Host	Host *V*	Period (d)	Radius (Jup)	Mass (Jup)	Discovery
KELT-9b	4050	A0	7.6	1.48	1.89	2.9	Gaudi et al. (2017)
WASP-33b	2780	A5	8.3	1.22	1.60	2.1	Collier Cameron et al. (2010)
Kepler-13b	2750	A2	10.0	1.76	1.41	∼9	Shporer et al. (2011)
WASP-189b	2640	A6	6.6	2.72	1.40	1.9	Anderson et al. (2018)
WASP-12b	2590	G0	11.7	1.09	1.90	1.5	Hebb et al. (2009)
MASCARA-1b	2570	A8	8.3	2.15	1.50	3.7	Talens et al. (2017)
HAT-P-70b	2560		9.5	2.74	1.87		Zhou et al. (2019)
WASP-103b	2510	F8	12.0	0.92	1.53	1.5	Gillon et al. (2014)
WASP-178b	2470	A1	9.9	3.34	1.81	1.7	This work
WASP-78b	2470	F8	12.0	2.17	2.06	0.9	Smalley et al. (2012)
KELT-16b	2450	F7	11.9	0.97	1.42	2.7	Oberst et al. (2017)
WASP-18b	2410	F9	9.3	0.94	1.20	10.5	Hellier et al. (2009)
WASP-121b	2360	F6	10.4	1.27	1.87	1.2	Delrez et al. (2016)
WASP-167b/KELT-13b	2330	F1	10.5	2.02	1.51		Temple et al. (2017)
WASP-87Ab	2320	F5	10.7	1.68	1.39	2.2	Anderson et al. (2014)

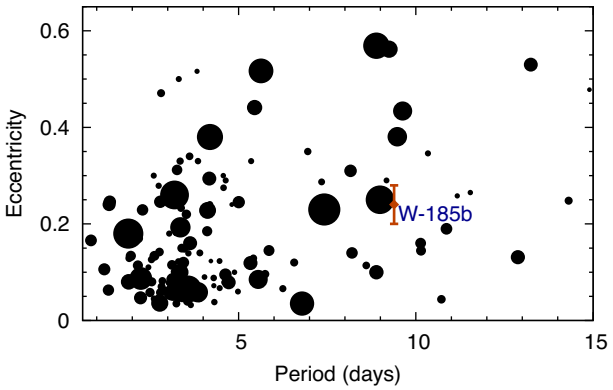

Figure 7. Orbital eccentricity versus orbital period for hot Jupiters, with WASP-185b's location in red. Only systems with $e > 0.03$ are shown. The symbol area scales with the planet mass. Data are from http://exoplanet.eu.

data from TEPcat[2], since it can be calculated uniformly for all the known systems. WASP-178b now joins this group. Transiting a $V = 9.95$ star, it is among the best UHJ targets visible from the Southern hemisphere, along with WASP-18b, WASP-103b, WASP-121b, and WASP-189b.

A correlation between high irradiation of hot Jupiters and bloated radii is now well established (e.g. Bhatti et al. 2016; Hartman et al. 2016; Sestovic, Demory & Queloz 2018). WASP-178b is at the upper end of such a relationship, as illustrated for known planets in Fig. 6. Also apparent in Table 7 is a tendency for the hottest hot Jupiters to be more massive than typical. The median mass of a transiting hot Jupiter is ∼0.9 $M_{\rm Jup}$, whereas the median of those in Table 7 is 2.2 $M_{\rm Jup}$. This presumably reflects the destruction of irradiated gas giants by photoevaporation (e.g. Owen & Lai 2018), such that lower-mass UHJs would have short lifetimes. Indeed, lower-mass UHJs such as WASP-12b (1.5 $M_{\rm Jup}$) are seen to be losing mass (e.g. Fossati et al. 2013). With a moderate mass of 1.7 $M_{\rm Jup}$, WASP-178b is thus also a candidate for photoevaporation.

We turn now to WASP-185b, which is notable for its eccentric orbit of $e = 0.24$. The tidal circularization time-scale increases markedly with orbital period, and so eccentric orbits are more likely for longer periods such as WASP-185b's 9.39 d (see Fig. 7). Using equation (3) of Adams & Laughlin (2006) we can estimate the circularization time-scale of WASP-185b as ∼2 Gyr, though this depends on assuming $Q_{\rm P} \sim 10^5$, which is uncertain. There is a tendency, however, for hot Jupiters with eccentric orbits to be either more massive (e.g. WASP-8b at 2.2 $M_{\rm Jup}$, Queloz et al. 2010; WASP-162b at 5.2 $M_{\rm Jup}$, Hellier et al. 2019a; and HAT-P-34b at 3.3 $M_{\rm Jup}$, Bakos et al. 2012) or to have indications of additional bodies in the system that might be perturbing the hot Jupiter (e.g. HAT-P-31b,c, Kipping et al. 2011; and HAT-P-17b,c, Howard et al. 2012). Given that WASP-185b is only 1 $M_{\rm Jup}$, and so should circularize more rapidly, and given the relatively long 6.6 ± 1.6 Gyr age of the host star, it may be that WASP-185b has arrived in its current orbit more recently, or that it is being perturbed by an outer companion (e.g. Petrovich & Tremaine 2016), possibly the putative companion at 1200 au. It would thus be worthwhile to obtain Rossiter–McLaughlin observations of WASP-185b to discern whether the planet's orbit is aligned or misaligned with the stellar rotation.

[2]https://www.astro.keele.ac.uk/jkt/tepcat/ (Southworth 2011).

ACKNOWLEDGEMENTS

WASP-South was hosted by the South African Astronomical Observatory and we are grateful for their support and assistance. Funding for WASP came from consortium universities and from the UK's Science and Technology Facilities Council. The Euler Swiss telescope is supported by the Swiss National Science Foundation. The research leading to these results has received funding from the ARC grant for Concerted Research Actions, financed by the Wallonia-Brussels Federation. TRAPPIST-South is funded by the Belgian Fund for Scientific Research (Fond National de la Recherche Scientifique, FNRS) under the grant FRFC 2.5.594.09.F, with the participation of the Swiss National Science Foundation (SNF). MG and EJ are F.R.S.-FNRS Senior Research Associates.

REFERENCES

Adams F. C., Laughlin G., 2006, ApJ, 649, 1004
Anderson D. R. et al., 2012, MNRAS, 422, 1988
Anderson D. R. et al., 2014, preprint (arXiv:1410.3449)
Anderson D. R. et al., 2018, preprint (arXiv:1809.04897)
Arcangeli J. et al., 2019, A&A, 625, A136
Bakos G. Á. et al., 2012, AJ, 144, 19
Barkaoui K. et al., 2019, AJ, 157, 43
Bhatti W. et al., 2016, preprint (arXiv:1607.00322)
Blackwell D. E., Shallis M. J., 1977, MNRAS, 180, 177
Boyajian T. S. et al., 2013, ApJ, 771, 40
Claret A., 2000, A&A, 363, 1081
Collier Cameron A. et al., 2007a, MNRAS, 375, 951
Collier Cameron A. et al., 2007b, MNRAS, 380, 1230
Collier Cameron A. et al., 2010, MNRAS, 407, 507
Delrez L. et al., 2016, MNRAS, 458, 4025
Doyle A. P. et al., 2013, MNRAS, 428, 3164
Doyle A. P., Davies G. R., Smalley B., Chaplin W. J., Elsworth Y., 2014, MNRAS, 444, 3592
Fossati L., Ayres T. R., Haswell C. A., Bohlender D., Kochukhov O., Flöer L., 2013, ApJ, 766, L20
Gaia Collaboration et al., 2016, A&A, 595, A1
Gaia Collaboration et al., 2018, A&A, 616, A1
Gaudi B. S. et al., 2017, Nature, 546, 514
Gillon M. et al., 2013, A&A, 552, A82
Gillon M. et al., 2014, A&A, 562, L3
Hartman J. D. et al., 2016, AJ, 152, 182
Hebb L. et al., 2009, ApJ, 693, 1920
Hellier C. et al., 2009, Nature, 460, 1098
Hellier C. et al., 2019a, MNRAS, 482, 1379
Hellier C. et al., 2019b, MNRAS, 488, 3067
Howard A. W. et al., 2012, ApJ, 749, 134
Kipping D. M. et al., 2011, AJ, 142, 95
Kreidberg L. et al., 2018a, AJ, 156, 17
Kreidberg L., Line M. R., Thorngren D., Morley C. V., Stevenson K. B., 2018b, ApJ, 858, L6
Lendl M. et al., 2012, A&A, 544, A72
Lund M. B. et al., 2017, AJ, 154, 194
Maxted P. F. L. et al., 2011, PASP, 123, 547
Maxted P. F. L., Serenelli A. M., Southworth J., 2015, A&A, 575, A36
Niemczura E., Smalley B., Pych W., 2014, Determination of Atmospheric Parameters of B-, A-, F- and G-Type Stars. Springer International Publishing, Cham, Switzerland
Oberst T. E. et al., 2017, AJ, 153, 97
Owen J. E., Lai D., 2018, MNRAS, 479, 5012
Parmentier V. et al., 2018, A&A, 617, A110
Pepe F., Mayor M., Galland F., Naef D., Queloz D., Santos N. C., Udry S., Burnet M., 2002, A&A, 388, 632
Petrovich C., Tremaine S., 2016, ApJ, 829, 132
Pollacco D. L. et al., 2006, PASP, 118, 1407
Queloz D. et al., 2001, A&A, 379, 279

Queloz D. et al., 2010, A&A, 517, L1
Ricker G. R. et al., 2016, Proc. SPIE, 9904, 99042B
Sestito P., Randich S., 2005, A&A, 442, 615
Sestovic M., Demory B.-O., Queloz D., 2018, A&A, 616, A76
Shporer A. et al., 2011, AJ, 142, 195
Smalley B. et al., 2012, A&A, 547, A61
Smith A. M. S. et al., 2012, AJ, 143, 81
Southworth J., 2011, MNRAS, 417, 2166
Stassun K. G., Torres G., 2018, ApJ, 862, 61
Talens G. J. J. et al., 2017, A&A, 606, A73
Talens G. J. J. et al., 2018, A&A, 612, A57
Temple L. Y. et al., 2017, MNRAS, 471, 2743
Triaud A. H. M. J. et al., 2013, A&A, 551, A80
Weiss A., Schlattl H., 2008, Ap&SS, 316, 99
Zhou G. et al., 2019, AJ, 158, 141

APPENDIX A

Table A1. Radial velocities (RVs).

BJD – 240 0000 (UTC)	RV (km s^{-1})	σ_{RV} (km s^{-1})	Bisector (km s^{-1})
WASP-178			
57850.91018	– 24.0725	0.0192	– 0.3486
57893.80235	– 23.8966	0.0426	– 0.2225
57894.56659	– 24.0744	0.0285	– 0.4313
57904.73294	– 24.0182	0.0364	– 0.2893
57934.67540	– 23.9881	0.0360	– 0.4670
57949.66427	– 23.7647	0.0545	– 0.3473
57951.58735	– 24.0164	0.0675	– 0.1183
57952.64066	– 23.8640	0.0377	– 0.3355
57954.60536	– 24.0314	0.0319	– 0.3859
57955.60534	– 23.8620	0.0957	– 0.1964
57958.65602	– 23.9400	0.0843	– 0.2004
57959.60533	– 23.7802	0.0220	– 0.3087
57974.59726	– 23.9948	0.0316	– 0.1979
58002.52881	– 23.8935	0.0367	– 0.4032
58018.48523	– 24.0258	0.0345	– 0.3217
58020.49026	– 23.8387	0.0359	– 0.2958
58030.48938	– 23.8311	0.0320	– 0.3998
58203.89388	– 23.7806	0.0299	– 0.3586
58207.82049	– 23.8350	0.0322	– 0.4199
58247.69603	– 23.8210	0.0366	– 0.2646
58276.47209	– 24.0082	0.0590	– 0.4419
58277.49486	– 23.6794	0.0367	– 0.4725
58320.57235	– 23.7790	0.0367	– 0.3855
WASP-184			
57190.68828	8.3083	0.0564	0.0095
57618.50533	8.4188	0.0306	0.0288
57817.78113	8.2765	0.0317	– 0.0066
57905.73109	8.3261	0.0273	0.0545
57924.47781	8.4413	0.0312	0.0950
57933.67645	8.4528	0.0730	0.0404
57954.53219	8.4176	0.0317	0.0363
57959.56409	8.4350	0.0347	– 0.0586
58170.79185	8.3245	0.0323	– 0.0012
58171.73350	8.3443	0.0372	– 0.1005
58172.74625	8.3889	0.0350	– 0.1351
58173.88416	8.3900	0.0292	0.0547
58174.70319	8.3157	0.0400	– 0.0645
58175.72199	8.3224	0.0337	0.0258
58247.77332	8.3381	0.0419	– 0.0371
58277.47072	8.3834	0.0384	0.0459
58307.53963	8.4145	0.0284	– 0.0570
58308.56619	8.3448	0.0482	0.2351
58309.57037	8.3142	0.0291	0.0041
58593.66628	8.0600	0.0625	0.0982
WASP-185			
57191.68952	23.7717	0.0243	– 0.0183
57193.69299	23.7864	0.0248	– 0.0048
57194.58975	23.8364	0.0150	0.0324
57218.60712	23.8076	0.0267	– 0.0193
57221.56637	23.7937	0.0160	0.0179
57412.87431	23.9926	0.0187	0.0396
57487.74786	23.9708	0.0106	0.0601
57488.68674	23.9470	0.0089	0.0051
57591.52359	23.9950	0.0116	0.0061
57599.55951	23.9768	0.0102	0.0201
57809.83999	23.8754	0.0105	– 0.0063
57815.86446	23.9621	0.0099	0.0093
57820.70709	23.8470	0.0114	0.0043
57901.58066	23.9342	0.0143	– 0.0072
57905.75841	23.8140	0.0123	0.0364
57918.49287	23.9202	0.0122	0.0222
57933.62653	23.7907	0.0239	– 0.0183
57951.54401	23.8020	0.0213	0.0090
57952.60960	23.7811	0.0148	0.0286
57990.48949	23.7948	0.0196	– 0.0256
58311.55039	23.8551	0.0147	0.0610
58312.57675	23.8646	0.0148	0.0097
58324.57747	23.8505	0.0198	– 0.0167
58357.50144	23.8219	0.0153	– 0.0224
WASP-192			
57568.61900	15.5839	0.0340	– 0.0655
58312.63770	16.2129	0.0304	– 0.0336
58329.60684	16.0837	0.0331	– 0.0253
58541.83740	15.6896	0.0533	0.1255
58542.87037	16.2018	0.0453	– 0.0570
58543.80761	15.8034	0.0445	– 0.0852
58544.74536	15.6832	0.0514	– 0.0766
58544.88449	15.7419	0.0518	0.1486
58545.72117	16.1702	0.1396	0.2143
58576.82272	15.9405	0.0537	0.0655
58576.88842	15.9702	0.0671	– 0.0397
58578.83595	15.5516	0.0611	0.0154

Note. Bisector errors are twice RV errors.

This paper has been typeset from a TEX/LATEX file prepared by the author.